Guises of Gouy:

Pang, X.

2013

Chapter 4

A generalized Gouy phase for focused, partially coherent wavefields and its implications for optical metrology

This Chapter is based on

- X. Pang, D.G. Fischer and T.D. Visser,
  "Generalized Gouy phase for focused, partially coherent light and its implications for optical metrology,"
  J. Opt. Soc. Am. A., vol. 29, pp. 989-993 (2012).

Abstract
When a monochromatic wavefield is focused, its phase, compared to that of a non-diffracted spherical wave, undergoes a rapid π phase change. This effect bears the name of its discoverer, L.G. Gouy. In a partially coherent wavefield the phase is a random quantity and therefore, when such a field is focused, its Gouy phase is undefined. However, the phase of the correlation functions that characterize partially coherent fields, such as the cross-spectral density and the spectral degree of coherence, *do* have

a well-defined phase. By introducing a generalized Gouy phase that is a function of two positions, we demonstrate that the correlation functions also undergo a rapid π phase change near focus. The dependence of this phenomenon on the state of coherence is examined. It is shown that in the coherent limit this generalized Gouy phase reduces to the classical Gouy phase. The implications for practical applications such as interference microscopy are examined. It is found that the fringe spacing is strongly influenced by the state of coherence.

4.1 Introduction

Traditionally, the Gouy phase is defined as the phase difference between a deterministic monochromatic, focused field and a plane wave or a non-diffracted spherical wave with the same frequency (see [Visser and Wolf, 2010] and the references therein). In practice, however, the field is often partially coherent, such as light that is produced by a multi-mode laser, or light that has traveled through the atmosphere or biological tissue. In those cases the phase of the wave field is a random quantity, and hence the Gouy phase is undefined in this situation.

In the space-frequency domain, partially coherent wavefields are characterized by correlation functions such as the cross-spectral density and the spectral degree of coherence [Mandel and Wolf, 1995]. In contrast to the field, these complex-valued functions typically have a well-defined phase. By introducing a generalized Gouy phase we show that the correlation functions exhibit a phase anomaly near focus that is remarkably similar to the rapid π phase change that occurs in focused, deterministic wavefields and in the coherent limit the generalized Gouy phase reduces to the classical phase anomaly. The phase behavior of the two-point correlation functions plays a central role in interference effects. We find that the fringe spacing that is observed in a Linnik interferometer is influenced by the state of coherence in a non-trivial manner. The focusing of partially coherent light has been examined by several authors and is reviewed in [Gbur and Visser, 2010]. Whereas most such studies deal with intensity distributions, in this chapter we will be concerned with the behavior of correlation functions.

4.2 Fully coherent focused fields

Let us first consider a converging, monochromatic field of frequency ω that emerges from a circular aperture with radius a (see Fig. 4.1). The origin O of the coordinate system is taken at the geometrical focus. The amplitude of the field in the aperture is $U^{(0)}(\mathbf{r}', \omega)$, with $\mathbf{r}'$ the position vector of a point $Q(\mathbf{r}')$. According to the Huygens-Fresnel principle, the field at a point $P(\mathbf{r})$ near focus can be expressed as ([Born and Wolf, 1999],

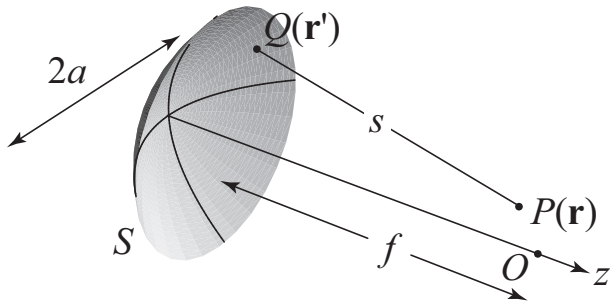

Figure 4.1: Illustrating the notation.

Sec. 8.8)

$$U(\mathbf{r},\omega) = -\frac{\mathrm{i}}{\lambda}\int_S U^{(0)}(\mathbf{r}',\omega)\frac{\exp(\mathrm{i}ks)}{s}\ \mathrm{d}^2r', \tag{4.1}$$

where the integration extends over the spherical wavefront S that fills the aperture, $s = |\mathbf{r} - \mathbf{r}'|$ denotes the distance QP, λ is the wavelength and $k = 2\pi/\lambda$ is the wavenumber associated with frequency ω. Using the Debye approximation one can derive for the space-dependent part of the field the expression ([Born and Wolf, 1999], Sec. 8.8)

$$U(x,y,z) = -\mathrm{i}k\frac{a^2}{f^2}Ce^{\mathrm{i}kz}\int_0^1 J_0\left(k\frac{a}{f}\sqrt{x^2+y^2}\ \rho\right)e^{-\mathrm{i}kz\rho^2a^2/2f^2}\ \rho\ \mathrm{d}\rho, \tag{4.2}$$

where f denotes the radius of the wavefront, C is a positive constant, and J_0 is the Bessel function of the first kind and zero order. For axial points ($x = y = 0$), Eq. (4.2) reduces to

$$\begin{aligned} U(0,0,z) &= -\mathrm{i}k\frac{a^2}{f^2}Ce^{\mathrm{i}kz}\int_0^1 e^{-\mathrm{i}kz\rho^2a^2/2f^2}\ \rho\ \mathrm{d}\rho, &(4.3)\\ &= -\mathrm{i}k\frac{a^2C}{2f^2}\mathrm{sinc}\left(kz\frac{a^2}{4f^2}\right)e^{\mathrm{i}kz(1-a^2/4f^2)}, &(4.4)\end{aligned}$$

where $\mathrm{sinc}(x) \equiv \sin(x)/x$. The argument (or "phase") of the field is therefore given by the expression

$$\arg[U(0,0,z)] = \begin{cases} -\dfrac{\pi}{2} + kz\left(1 - \dfrac{a^2}{4f^2}\right) \pmod{2\pi}\ ^{1}, & \text{if } \mathrm{sinc}\left(kz\dfrac{a^2}{4f^2}\right) > 0, \\ \dfrac{\pi}{2} + kz\left(1 - \dfrac{a^2}{4f^2}\right) \pmod{2\pi}, & \text{if } \mathrm{sinc}\left(kz\dfrac{a^2}{4f^2}\right) < 0. \end{cases} \tag{4.5}$$

Since

$$\mathrm{sinc}\left(kz\frac{a^2}{4f^2}\right) > 0, \qquad \text{if } |z| < 2\lambda f^2/a^2, \tag{4.6}$$

the phase of the field in the immediate vicinity of the focus can be written as

$$\arg[U(0,0,z)] = -\frac{\pi}{2} + kz\left(1 - \frac{a^2}{4f^2}\right). \tag{4.7}$$

It follows from Eq. (4.7) that on the optical axis the phase changes *slower* than that of a plane wave of the same frequency[2]: The effective wavelength near focus equals $\lambda/(1 - a^2/4f^2)$.

The Gouy phase $\delta(z)$ of a focused, monochromatic field at an axial point $\mathbf{r} = (0,0,z)$ is defined as the difference between the argument of the field $U(0,0,z)$ and that of a plane wave of the same frequency, i.e.

$$\delta(z) \equiv \arg[U(0,0,z)] - kz \pmod{2\pi}. \tag{4.8}$$

On substituting from Eq. (4.7) into Eq. (4.8) we find that

$$\delta(0) = -\pi/2. \tag{4.9}$$

Furthermore, the Gouy phase has the symmetry property

$$\delta(z) + \delta(-z) = -\pi, \tag{4.10}$$

[1] The symbol mod 2π denotes that the two sides of the equation are indeterminate to the extent of an additive constant $2m\pi$ where m is any integer.

[2] This was first derived in [Linfoot and Wolf, 1956], but on page 828 it is erroneously stated that "the equiphase surfaces are spaced *closer* together, by a factor $1 - a^2/4f^2$ ...".

and its derivative of near focus is given by the expression

$$\frac{\mathrm{d}\delta(z)}{\mathrm{d}z} = -k\frac{a^2}{4f^2} \quad [\mathrm{rad/m}]. \tag{4.11}$$

An example of the behavior of the Gouy phase is shown in Fig. 4.2. The discontinuities by an amount of π occur at the zeros (or phase singularities) of the field.

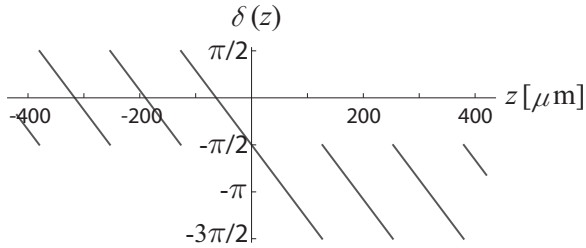

Figure 4.2: The classical Gouy phase $\delta(z)$ along the optical axis for a deterministic (i.e., fully coherent) focused wave field. In this example $a = 1$ cm, $f = 10$ cm and $\lambda = 0.6328$ μm.

4.3 Partially coherent focused fields

For a partially coherent wave field one must consider, instead of the stochastic amplitude $U^{(0)}(\mathbf{r}', \omega)$, the cross-spectral density function ([Mandel and Wolf, 1995], Sec. 2.4) of the field at two points $Q_1(\mathbf{r}'_1)$ and $Q_2(\mathbf{r}'_2)$, namely,

$$W^{(0)}(\mathbf{r}'_1, \mathbf{r}'_2, \omega) = \langle {U^{(0)}}^*(\mathbf{r}'_1, \omega) U^{(0)}(\mathbf{r}'_2, \omega) \rangle. \tag{4.12}$$

Here the angled brackets denote the average, take over a statistical ensemble of monochromatic realizations $\{U^{(0)}(\mathbf{r}', \omega) \exp(-\mathrm{i}\omega t)\}$ ([Mandel and Wolf, 1995], Sec. 4.7) and the asterisk denotes the complex conjugate. The cross-spectral density of the focused field is given by the similar expression

$$W(\mathbf{r}_1, \mathbf{r}_2, \omega) = \langle U^*(\mathbf{r}_1, \omega) U(\mathbf{r}_2, \omega) \rangle. \tag{4.13}$$

On substituting from Eq. (4.1) into Eq. (4.13) we find that

$$W(\mathbf{r}_1,\mathbf{r}_2,\omega)=\frac{1}{\lambda^2}\int_S\int_S W^{(0)}(\mathbf{r}',\mathbf{r}'',\omega)\frac{e^{\mathrm{i}k(s_2-s_1)}}{s_1 s_2}\,\mathrm{d}^2r'\mathrm{d}^2r'', \tag{4.14}$$

with

$$s_1 = \left|\mathbf{r}_1-\mathbf{r}'\right|, \tag{4.15}$$
$$s_2 = \left|\mathbf{r}_2-\mathbf{r}''\right|. \tag{4.16}$$

From now on we omit the dependence of the various quantities on the frequency ω. We assume that the field in the aperture is a Gaussian Schell-model field ([Mandel and Wolf, 1995], Sec. 5.4) with uniform intensity A^2, i.e.,

$$W^{(0)}(\mathbf{r}',\mathbf{r}'')=W^{(0)}(\boldsymbol{\rho}',\boldsymbol{\rho}'')=A^2e^{-(\boldsymbol{\rho}''-\boldsymbol{\rho}')^2/2\sigma^2}, \tag{4.17}$$

where $\boldsymbol{\rho}=(x,y)$ is a two-dimensional transverse vector and σ is a positive constant that is a measure of the effective transverse coherence length of the field.

In the following we restrict our attention to observation points on the z-axis, i.e. $\mathbf{r}_1=(0,0,z_1)$, $\mathbf{r}_2=(0,0,z_2)$. The factors s_i $(i=1,2)$ in the denominator of Eq. (4.14) can be approximated by the focal length f and in the exponent they may be approximated by the expressions

$$s_1 \approx f-\hat{\mathbf{q}}'\cdot\mathbf{r}_1, \tag{4.18}$$
$$s_2 \approx f-\hat{\mathbf{q}}''\cdot\mathbf{r}_2, \tag{4.19}$$

where $\hat{\mathbf{q}}'$ and $\hat{\mathbf{q}}''$ are unit vectors in the directions $O\mathbf{r}'$ and $O\mathbf{r}''$, respectively. In cylindrical coordinates ρ and ϕ we thus find that

$$\hat{\mathbf{q}}'\cdot\mathbf{r}_1 \approx -z_1(1-\rho'^2/2f^2), \tag{4.20}$$
$$\hat{\mathbf{q}}''\cdot\mathbf{r}_2 \approx -z_2(1-\rho''^2/2f^2). \tag{4.21}$$

On making use of these expressions, Eq. (4.14) becomes

$$W(z_1,z_2) = \left(\frac{A}{\lambda f}\right)^2\int_0^{2\pi}\int_0^a\int_0^{2\pi}\int_0^a e^{-[\rho'^2+\rho''^2-2\rho'\rho''\cos(\phi'-\phi'')]/2\sigma^2} \times e^{\mathrm{i}k[-z_1(1-\rho'^2/2f^2)+z_2(1-\rho''^2/2f^2)]}\rho'\rho''\mathrm{d}\phi'\mathrm{d}\rho'\mathrm{d}\phi''\mathrm{d}\rho'', \tag{4.22}$$

where we have used the relation $\mathrm{d}x\mathrm{d}y = \rho\ \mathrm{d}\rho\mathrm{d}\phi$. Since

$$\int_0^{2\pi}\int_0^{2\pi} e^{\rho'\rho''\cos(\phi'-\phi'')/\sigma^2}\ \mathrm{d}\phi'\mathrm{d}\phi'' = 4\pi^2 I_0\left(\frac{\rho'\rho''}{\sigma^2}\right), \tag{4.23}$$

with I_0 denoting the modified Bessel function of order zero, we finally obtain for the cross-spectral density the formula [Fischer and Visser, 2004]

$$\begin{aligned} W(z_1,z_2) \ &= \ A^2\frac{k^2}{f^2}\int_0^a\int_0^a e^{-(\rho''+\rho')^2/2\sigma^2} I_0\left(\frac{\rho'\rho''}{\sigma^2}\right) \\ &\quad \times e^{\mathrm{i}k[-z_1(1-\rho'^2/2f^2)+z_2(1-\rho''^2/2f^2)]}\rho'\rho''\mathrm{d}\rho'\mathrm{d}\rho''. \end{aligned} \tag{4.24}$$

The cross-spectral density can be normalized by defining the spectral degree of coherence as

$$\mu(z_1,z_2) \equiv \frac{W(z_1,z_2)}{[S(z_1)S(z_2)]^{1/2}}, \tag{4.25}$$

with the spectral density distribution $S(z) = W(z,z)$. Since $S(z)$ is a positive, real-valued function, the spectral degree of coherence $\mu(z_1,z_2)$ and the cross-spectral density $W(z_1,z_2)$ have the same phase.

4.4 A generalized Gouy phase

Let us introduce a *generalized Gouy phase* as the difference between the phase of the cross-spectral density $W(z_1,z_2)$ and the phase of $e^{\mathrm{i}k(z_2-z_1)}$, i.e.

$$\delta_\mu(z_1,z_2) = \arg[W(z_1,z_2)] - k(z_2-z_1) \pmod{2\pi}. \tag{4.26}$$

Here the subscript μ indicates that this definition pertains to the phase of the cross-spectral density or, equivalently, the spectral degree of coherence. The reference phases kz_1 and kz_2 are those of a plane wave of frequency $\omega = kc$, with c the speed of light, at positions z_1 and z_2, respectively. In contrast to the classical Gouy phase, definition (4.26) involves the phase of a two-point correlation function rather than that of a deterministic wave field that only depends on a single spatial variable. In addition, two reference phases are taken into account instead of one.

Let us take the first observation point at origin O, i.e., $z_1 = 0$. The cross-spectral density of Eq. (4.24) now becomes

$$W(0, z_2) = A^2 \frac{k^2}{f^2} \int_0^a \int_0^a e^{-(\rho'' + \rho')^2/2\sigma^2} I_0\left(\frac{\rho' \rho''}{\sigma^2}\right) e^{\mathrm{i}kz_2(1-\rho''^2/2f^2)} \rho' \rho'' \mathrm{d}\rho' \mathrm{d}\rho'', \tag{4.27}$$

and Eq. (4.26) reduces to

$$\delta_\mu(0, z_2) = \arg\left[\int_0^a \int_0^a e^{-(\rho'' + \rho')^2/2\sigma^2} I_0\left(\frac{\rho' \rho''}{\sigma^2}\right) e^{-\mathrm{i}kz_2\rho''^2/2f^2} \rho' \rho'' \mathrm{d}\rho' \mathrm{d}\rho''\right]. \tag{4.28}$$

Examples of the generalized Gouy phase are shown in Fig. 4.3 for different values of the normalized transverse coherence length σ/a. It is seen that $\delta_\mu(0, z_2)$ exhibits an anomalous phase behavior that is quite similar to that of deterministic fields, with the phase near focus undergoing a rapid phase change of π. In addition, the generalized Gouy phase obeys the following relations:

$$\delta_\mu(0, 0) = 0 \tag{4.29}$$

and

$$\delta_\mu(0, z_2) + \delta_\mu(0, -z_2) = 0, \tag{4.30}$$

which are the statistical analogs of Eqs. (4.9) and (4.10) for the deterministic case. In fact, apart from a $\pi/2$ offset, which can be traced back to the prefactor i in Eq. (4.1), they are identical.

On the other hand, there are some striking differences. For instance, the modulation depth of the generalized Gouy phase is dependent on the transverse coherence length of the incident field. It is small for incoherent fields and increases in size as the coherence length is increased. In addition, the generalized Gouy phase has regions of both positive and negative slope, unlike the coherent case for which the slope is always negative. The implications of this for interference experiments will be discussed shortly.

Next we show that the classical phase anomaly is a special case of the generalized Gouy phase. Repeating Eq. (4.13), we have that

$$W(z_1, z_2) = \langle U^*(z_1) U(z_2) \rangle. \tag{4.31}$$

When the field is deterministic, only a single realization exists and the cross-spectral density $W(z_1, z_2)$ factorizes into the form

$$W(z_1, z_2) = U^*(z_1) U(z_2). \tag{4.32}$$

In that case the Gouy phase expressed by Eq. (4.26) becomes

$$\delta_\mu(z_1, z_2) = \arg[U^*(z_1)] + \arg[U(z_2)] - k(z_2 - z_1) \pmod{2\pi}. \quad (4.33)$$

If we set $z_1 = 0$, we get

$$\delta_\mu(0, z_2) = \arg[U(z_2)] - kz_2 + \pi/2 \pmod{2\pi}, \quad (4.34)$$

where we made use of Eq. (4.4). It is seen that in this special case the generalized Gouy phase, apart from an inconsequential constant, reduces to the classical Gouy phase [given by Eq. (4.8)]. Furthermore, in the coherent limit ($\sigma \to \infty$) Eq. (4.28) can be solved analytically and we obtain the result that near $z = 0$

$$\delta_\mu(0, z_2) = -kz_2a^2/4f^2, \quad (4.35)$$

which is identical to the Gouy phase behavior of deterministic waves as discussed in connection with Fig. 4.2.

The behavior of the spectral degree of coherence has been studied by [Fischer and Visser, 2004]. An example, calculated from Eq. (4.25) is shown for pairs of axial points z_1 and z_2 in Fig. 4.4. It is seen that $|\mu(z_1, z_2)|$ is an oscillatory function of the distance $|z_1 - z_2|$.

Using Eq. (4.26) the generalized Gouy phase for axial points z_1 and z_2 is computed and displayed in Fig. 4.5. Here the value of the normalized coherence length $\sigma/a = 0.5$. In this plot the diagonal line denotes the Gouy phase of the cross-spectral density when $z_1 = z_2$. When the coherence length of the field increases, the different contour lines move closer together, as can be seen in Fig. 4.6 and Fig. 4.7.

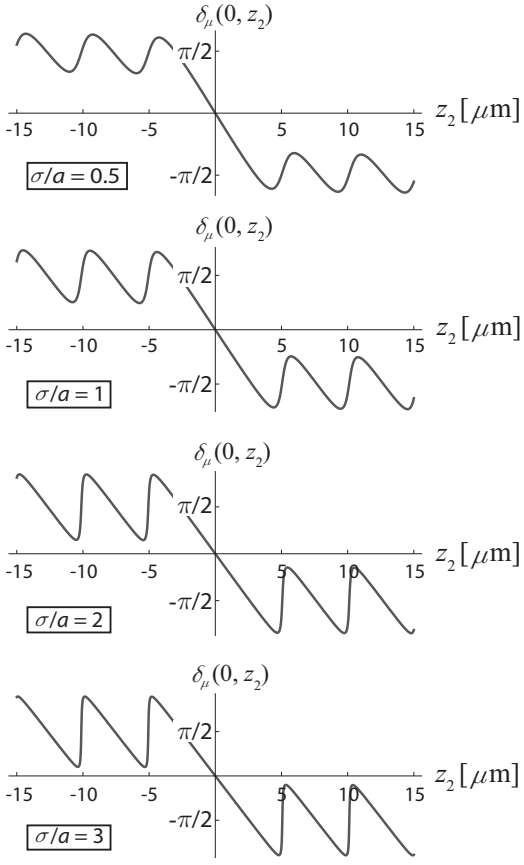

Figure 4.3: The generalized Gouy phase $\delta_\mu(0, z_2)$ of a focused partially coherent field for different values of the transverse coherence length of the field in the aperture. In these examples $a = 1$ cm, $f = 2$ cm, and $\lambda = 0.6328$ μm.

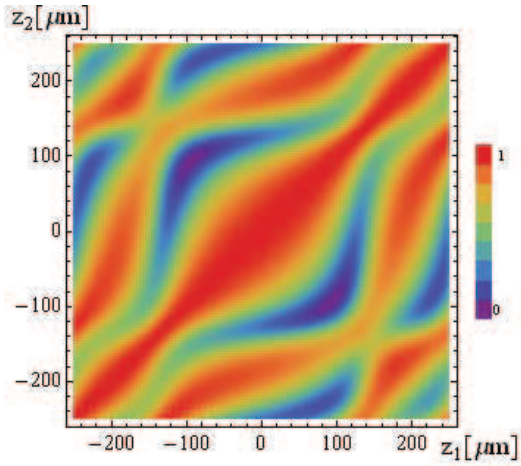

Figure 4.4: Color-coded plot of the modulus of the spectral degree of coherence, $|\mu(z_1, z_2)|$ when the incident field has a normalized coherence length $\sigma/a = 0.5$. In this example $a = 1$ cm, $f = 10$ cm, and $\lambda = 0.6328$ μm.

4.5 The origin of the generalized Gouy phase

The physical origin of the classical Gouy phase has been discussed in [Visser and Wolf, 2010]. In this section we show that a similar analysis explains the π phase change that the generalized Gouy phase undergoes near focus.

Consider an astigmatic surface S' with focal lines at C_1 and C_2. The point Q represents the intersection of S' and the z-axis (see Fig. 4.8), and is taken as the origin of the coordinate system. The two focal lengths are denoted by $f_1 = QC_1$ and $f_2 = QC_2$, respectively.

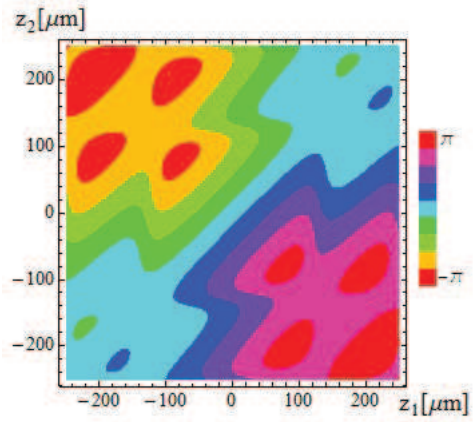

Figure 4.5: The generalized Gouy phase of the cross-spectral density for pairs of axial points z_1 and z_2 when the incident field has a normalized coherence length $\sigma/a = 0.5$. In this example $a = 1$ cm, $f = 10$ cm, and $\lambda = 0.6328$ μm.

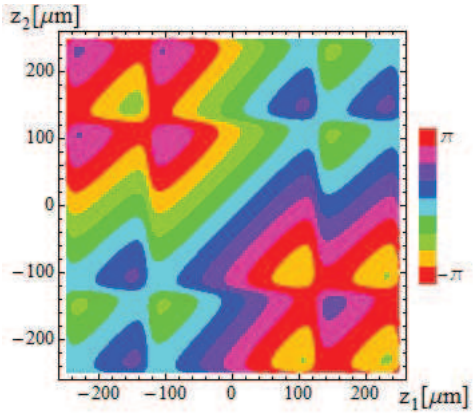

Figure 4.6: The generalized Gouy phase of the cross-spectral density for pairs of axial points z_1 and z_2 when the incident field has a normalized coherence length $\sigma/a = 1$. In this example $a = 1$ cm, $f = 10$ cm, and $\lambda = 0.6328$ μm.

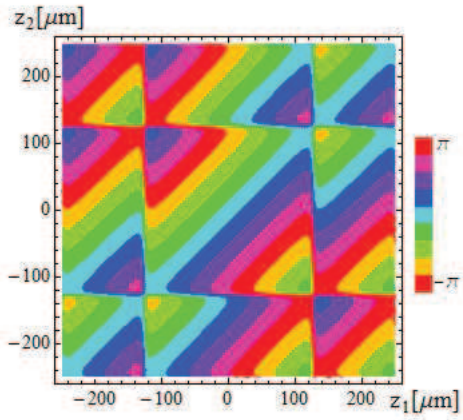

Figure 4.7: The generalized Gouy phase of the cross-spectral density for pairs of axial points z_1 and z_2 when the incident field has a normalized coherence length $\sigma/a = 2$. In this example $a = 1$ cm, $f = 10$ cm, and $\lambda = 0.6328$ μm.

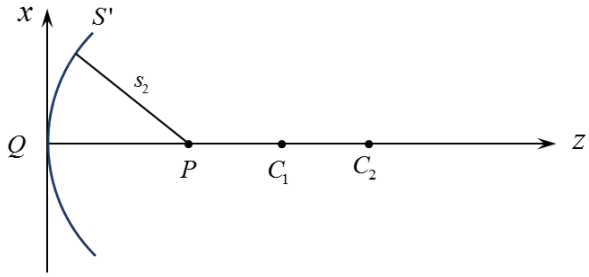

Figure 4.8: An astigmatic surface S' with focal lines at C_1 and C_2. The focal lengths $QC_1 = f_1$ and $QC_2 = f_2$. The distance from a point of integration on S' to the observation point P is denoted by s_2.

According to Eq. (4.14) the cross-spectral density can be written as

$$W(\mathbf{r}_1, \mathbf{r}_2) = \frac{1}{\lambda^2} \int_{S'} \int_{S'} W^{(0)}(\mathbf{r}', \mathbf{r}'') \frac{e^{ik(s_2 - s_1)}}{s_1 s_2} \, \mathrm{d}^2 r' \mathrm{d}^2 r'', \tag{4.36}$$

with s_1, s_2 given by Eqs. (4.15) and (4.16). If the distance between the two focal lines may be assumed to be small, we have that

$$\frac{1}{s_1} \approx \frac{1}{s_2} \approx \frac{1}{f}, \tag{4.37}$$

where

$$f = \frac{f_1 + f_2}{2}. \tag{4.38}$$

Hence

$$W(\mathbf{r}_1, \mathbf{r}_2) \approx \frac{1}{\lambda^2 f^2} \int_{S'} \int_{S'} W^{(0)}(\mathbf{r}', \mathbf{r}'') e^{\mathrm{i}k(s_2 - s_1)} \, \mathrm{d}^2 r' \mathrm{d}^2 r''. \tag{4.39}$$

The main contribution to this oscillatory integral comes from those points where s_1 and s_2 are stationary, i.e. in the vicinity of the point Q in Fig. 4.8. In that region the amplitude function $W^{(0)}(\mathbf{r}', \mathbf{r}'')$ may be approximated by the value $W^{(0)}(0, 0)$. Also, since only the immediate neighborhood around this stationary point contributes significantly to the integral, it is justified to expand the limits of the integration in Eq. (4.39) to minus and plus infinity. Thus we find that

$$W(\mathbf{r}_1, \mathbf{r}_2) \approx C_1 \frac{W^{(0)}(0, 0)}{\lambda^2 f^2} \int_{-\infty}^{\infty} e^{\mathrm{i}ks_2} \, \mathrm{d}^2 r'' \int_{-\infty}^{\infty} e^{-\mathrm{i}ks_1} \, \mathrm{d}^2 r', \tag{4.40}$$

with C_1 a constant [Stamnes, 1986].

Next we restrict ourselves to axial points, i.e. $\mathbf{r}_1 = (0, 0, z_1)$, $\mathbf{r}_2 = (0, 0, z_2)$. Then Eq. (4.40) can be written as

$$W(z_1, z_2) \approx C_2 \int_{-\infty}^{\infty} e^{\mathrm{i}ks_2} \, \mathrm{d}^2 r'' \int_{-\infty}^{\infty} e^{-\mathrm{i}ks_1} \, \mathrm{d}^2 r', \tag{4.41}$$

where C_2 is a constant. Let us first analyze the left-hand integral. Since the equation of the surface S' is approximately

$$z = \frac{x^2}{2f_1} + \frac{y^2}{2f_2}, \tag{4.42}$$

we have that

$$s_2 = \sqrt{x^2 + y^2 + (z_2 - z)^2}, \tag{4.43}$$

$$\approx z_2 + \alpha_1 x^2 + \alpha_2 y^2, \tag{4.44}$$

where

$$\alpha_1 = \frac{f_1 - z_2}{2f_1 z_2}, \tag{4.45}$$

$$\alpha_2 = \frac{f_2 - z_2}{2f_2 z_2}. \tag{4.46}$$

This way we find that

$$\int_{-\infty}^{\infty} e^{\mathrm{i}ks_2}\ \mathrm{d}^2 r'' \approx e^{\mathrm{i}kz_2} \int_{-\infty}^{\infty} e^{\mathrm{i}k(\alpha_1 x^2 + \alpha_2 y^2)}\ \mathrm{d}x\mathrm{d}y. \tag{4.47}$$

Now let us write $\xi = x\sqrt{k}$, $\mu = y\sqrt{k}$, then Eq. (4.47) becomes

$$\int_{-\infty}^{\infty} e^{\mathrm{i}ks_2}\ \mathrm{d}^2 r'' \approx e^{\mathrm{i}kz_2} \int_{-\infty}^{\infty} e^{\mathrm{i}\alpha_1 \xi^2}\ \mathrm{d}\xi \int_{-\infty}^{\infty} e^{\mathrm{i}\alpha_2 \mu^2}\ \mathrm{d}\mu. \tag{4.48}$$

Since

$$\int_{-\infty}^{\infty} e^{\pm \mathrm{i}t^2}\ \mathrm{d}t = (1 \pm i)\sqrt{\frac{\pi}{2}}, \tag{4.49}$$

we have that

$$\int_{-\infty}^{\infty} e^{\mathrm{i}\alpha\xi^2}\ \mathrm{d}\xi = (1 \pm i)\sqrt{\frac{\pi}{2|\alpha|}}, \tag{4.50}$$

according as α is positive or negative. Three cases can now be distinguished:

1) The point P lies to the left of C_1 and C_2, i.e., $z_2 < f_1 < f_2$. In this case $\alpha_1,\ \alpha_2 > 0$ and

$$\int_{S'} e^{\mathrm{i}ks_2}\ \mathrm{d}^2 r'' \approx \mathrm{i}2\pi z_2 e^{\mathrm{i}kz_2} \sqrt{\frac{f_1 f_2}{(f_1 - z_2)(f_2 - z_2)}}. \tag{4.51}$$

2) The point P is located between C_1 and C_2, i.e., $f_1 < z_2 < f_2$. In this case α_1 is negative and α_2 is positive, and

$$\int_{-\infty}^{\infty} e^{\mathrm{i}ks_2}\ \mathrm{d}^2 r'' \approx 2\pi z_2 e^{\mathrm{i}kz_2} \sqrt{\frac{-f_1 f_2}{(f_1 - z_2)(f_2 - z_2)}}. \tag{4.52}$$

3) The point P lies to the right of C_2, i.e., $z_2 > f_2 > f_1$. Then $\alpha_1,\ \alpha_2 < 0$, and

$$\int_{-\infty}^{\infty} e^{\mathrm{i}ks_2}\ \mathrm{d}^2r'' \approx -\mathrm{i}2\pi z_2 e^{\mathrm{i}kz_2}\sqrt{\frac{f_1 f_2}{(f_1 - z_2)(f_2 - z_2)}}. \tag{4.53}$$

A comparison of Eqs. (4.51), (4.52) and (4.53) shows that when the point P moves through the two focal lines at C_1 and C_2, the phase of the first integral of Eq. (4.41) twice jumps by an amount of $\pi/2$. If now we take the limit of the astigmatism going to zero, the surface S' becomes spherical and $f_1 = f_2 = f$. Also, the two successive $\pi/2$ phase jumps coincide to yield a single π phase jump.

When we set $z_1 = (f_2 + f_1)/2 = f$ the second integral becomes

$$\int_{-\infty}^{\infty} e^{-\mathrm{i}ks_1}\ \mathrm{d}^2r' = \int_{-\infty}^{\infty} e^{-\mathrm{i}kf}\ \mathrm{d}^2r' = \text{Constant}. \tag{4.54}$$

The value of this integral can be absorbed in a new constant C_3, and we obtain the expression

$$W(z_1, z_2) = C_3 \int_{-\infty}^{\infty} e^{\mathrm{i}ks_2}\ \mathrm{d}^2r''. \tag{4.55}$$

According to Eqs. (4.51)–(4.53), for a spherical surface the generalized Gouy phase undergoes a π phase jump, just like its classical counterpart. This discontinuous behavior is the result of the use of the method of stationary phase in which the limit $k \to \infty$ is studied. As is well known, this limit yields the results of geometrical optics. The actual field, however, satisfies the Helmholtz equation, the solutions of which are continuous. We can therefore expect the π phase jump to be "smoothed out" into a rapid, but continuous π phase change as is indeed seen in Fig. 4.3.

4.6 Implications for interferometry

It is well known that the fringe spacing in interference microscopy is typically irregular, and depends on both the numerical aperture and the apodization [Creath, 1989; Foley and Wolf, 2005]. It has also recently been established that the spatial coherence of the incident field plays a role, although its treatment has been empirical to date.

To quantitatively investigate the effects of spatial coherence on interference fringe spacing (and, ultimately, on interference metrology) and the role that the generalized Gouy phase plays, we consider the Linnik microscope [Kino and Korle, 1996]. Such microscope is a two-beam interferometer which is widely used for studying the structure of reflecting specimens. A sketch is shown in Fig. 4.9. In this figure, two identical microscope objectives are placed in each arm. In one arm a reference object is placed in the focal plane. In the other arm a test object can be scanned through the focus. The superposition of the two reflected beams is recorded as a function of the axial position z_2. The detected interference pattern is formed by the light emerging from the two axial points, $P_1 = (0, 0, 0)$, $P_2 = (0, 0, z_2)$. On making use of Eq. (4.25) we can write the spectral density of this superposition as

$$|U(0) + U(z_2)|^2 = S(0) + S(z_2) + 2\sqrt{S(0)S(z_2)}\mathrm{Re}[\mu(0, z_2)], \qquad (4.56)$$

which is commonly known as the *spectral interference law* [Mandel and Wolf, 1995, Sec. 4.3].

It is clear from Eq. (4.56) that in an interferogram, in which the spectral density of the superposition is recorded as a function of the distance z_2, the spacing of the ensuing fringe pattern is determined by $\mu(0, z_2)$, the spectral degree of coherence. When the field is fully coherent, the spectral density of the field can be expressed analytically from Eqs. (4.4), (4.32) and (4.56), as

$$\begin{aligned} S(M) \;=\; & C^2 \frac{k^2 a^4}{4f^4} + C^2 \frac{4}{z_2^2} \sin^2\left(k z_2 \frac{a^2}{4f^2}\right) \\ & + 2C^2 \frac{k a^2}{f^2 z_2} \sin\left(k z_2 \frac{a^2}{4f^2}\right) \cos\left[k z_2 (1 - \frac{a^2}{4f^2})\right]. \end{aligned} \qquad (4.57)$$

While for a partially coherent field, such as in our model, $\mu(0, z_2)$ is characterized by a single parameter, namely the transverse coherence length σ of the field in the aperture. As was seen in Fig. 4.3, this parameter has a significant influence on the phase behavior of the spectral degree of coherence near focus.

For low NA fields, $S(z_2)$ is a slowly varying function compared to $\mu(0, z_2)$, which varies sinusoidally on the scale of the wavelength. For

high NA fields, however, $S(z_2)$ changes much faster and the maxima of the interference term in Eq. (4.56) are no longer coincident with those of $\mathrm{Re}[\mu(0, z_2)]$.

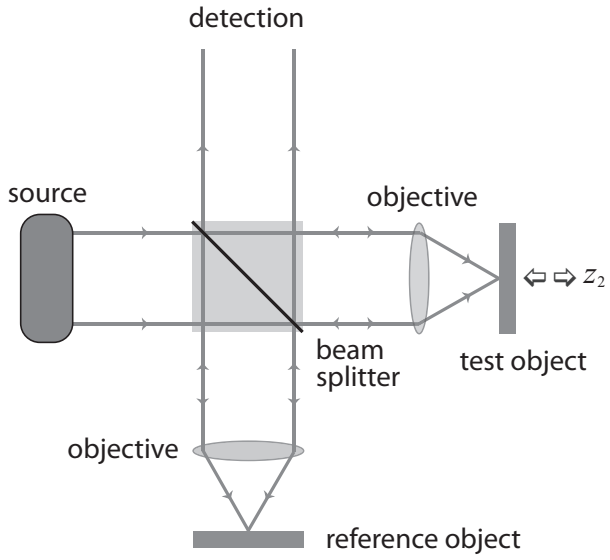

Figure 4.9: Sketch of a Linnik interferometer.

To quantify the effect of the state of coherence of the incident field on the interference process, we have computed the spacing of the fringes for three cases, each with the same (relatively high) numerical aperture and varying degrees of spatial coherence: $\sigma/a = 0.5$, $\sigma/a = 1$, and $\sigma/a = 50$. The results are listed in Table 4.1 for the first 11 fringes.

As can be seen, in all three cases, the spacings of the first several fringes, which are primarily dictated by $\mu(0, z_2)$, are larger than the free-space wavelength. This increased spacing was discussed earlier for the coherent case, and is due to the behavior of the Gouy phase. Accordingly, if the fringe spacings were due solely to $\mu(0, z_2)$, we would expect, in coherent case, that they would be identical except when the region between the corresponding intensity maxima contains a phase discontinuity of the Gouy phase. That this is not the case is due to the fact that the spectral density $S(z_2)$ modulates the spectral degree of coherence [in Eq. (4.56)]

and displaces additional maxima in the neighborhood of the discontinuities. By contrast, for the partially coherent cases, a greater number of fringes are inherently affected near the phase jumps of the generalized Gouy phase. This is because the transition at the jumps is more gradual (i.e. not a true discontinuity). Furthermore, as the field becomes less coherent, the size of the jumps (i.e. the modulation depth) decreases and the transition near the jumps becomes smoother. Therefore, the fringe spacing is highly irregular in all three cases, with the maximum fringe displacement (♯8) occurring for the coherent case ($\sigma/a = 50$) and the maximum fringe variation (greater number of affected fringes) and smallest fringe displacement occurring for the least coherent case. The maximum fringe displacements, given by the 8^{th} fringe in each case, are 0.5944, 0.5579, and 0.4647, from least coherent to most coherent.

Table 4.1: Fringe spacings for three values of the transverse coherence length σ. In all cases the aperture radius $a = 1$ cm, the focal length $f = 2$ cm,and the free-space wavelength is $\lambda = 0.6328$ μm.

♯	$\sigma/a = 0.5$	$\sigma/a = 1$	$\sigma/a = 50$
1	0.6675	0.6702	0.6730
2	0.6671	0.6699	0.6730
3	0.6662	0.6695	0.6730
4	0.6642	0.6683	0.6729
5	0.6602	0.6657	0.6724
6	0.6509	0.6582	0.6702
7	0.6284	0.6311	0.6560
8	0.5944	0.5579	0.4647
9	0.6044	0.5926	0.5975
10	0.6368	0.6465	0.6652
11	0.6519	0.6601	0.6704

In Figs. 4.10 and 4.11, we have plotted the interferograms corresponding to the first and third cases in Table 4.1 ($\sigma/a = 0.5$ and $\sigma/a = 50$).

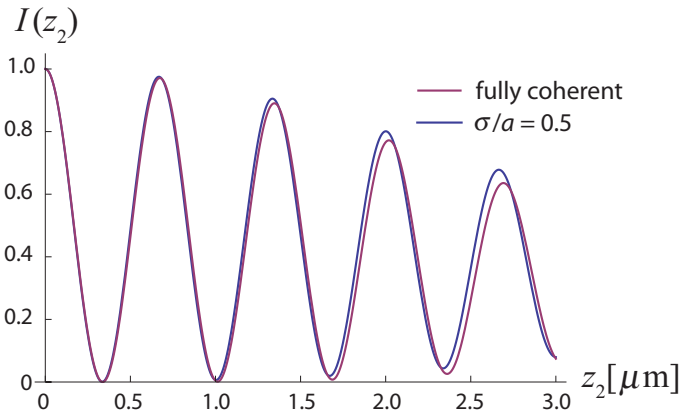

Figure 4.10: Interferogram for a fully coherent field ($\sigma/a = 50$) (red curve), and for a partially coherent field ($\sigma/a = 0.5$) (blue curve). In both cases $a = 1$ cm, $f = 2$ cm, and $\lambda = 0.6328$ μm.

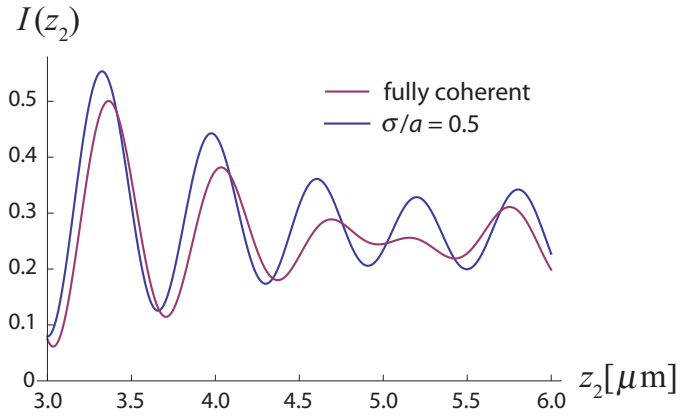

Figure 4.11: Same as Figure 4.10, but for larger values of the axial position z_2.

It is seen from Fig. 4.10 that the fringe spacing of the fully coherent field (red curve) is initially somewhat larger than that of the partially coherent field (blue curve). However, Fig. 4.11 shows that for larger values of z_2 the fringes of the fully coherent field move closer together and the

maxima of the fringe pattern go from trailing the partially coherent case to leading it. This transition occurs around $z_2 = 4.5$ μm, which is precisely the point where the slope of the generalized Gouy phase changes from being negative to being positive (see the top panel of Fig. 4.3). Near $z_2 = 6.0$ μm the sign of the slope changes again and fringe spacing of the partially coherent field again becomes smaller than that of the fully coherent field. The slope of the classical Gouy phase (as shown in Fig. 4.12) is, apart from the discontinuities at the axial phase singularities, always negative. Therefore such an effect does not occur for coherent fields.

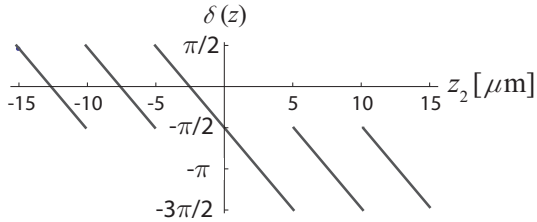

Figure 4.12: The generalized Gouy phase $\delta_\mu(0, z_2)$ of a fully coherent field. In this example $a = 1$ cm, $f = 2$ cm, and $\lambda = 0.6328$ μm.

4.7 Conclusions

We have defined a generalized Gouy phase for partially coherent fields. In contrast to its traditional counterpart, this phase pertains to the spectral degree of coherence, a two-point correlation function, rather than to the phase of a deterministic wave field that depends only an a single point. It was shown that the classical phase anomaly is a special case of the generalized Gouy phase. The generalized Gouy phase was examined numerically and analytically for the broad class of Gaussian-correlated fields. It was demonstrated that our findings have important implications for metrology with partially coherent fields.